The Journal of Chemical Physics

RESEARCH ARTICLE | FEBRUARY 04 2026

Observation of Penning electron detachment by electronically excited potassium atoms in high Rydberg states FREE

Tatsuya Chiba ; Moritz Blankenhorn ; Shiying Wang ; Burak A. Tufekci ; Kathryn Foreman ; Kit H. Bowen

J. Chem. Phys. 164, 054312 (2026)
https://doi.org/10.1063/5.0311876

The Journal of Chemical Physics ARTICLE pubs.aip.org/aip/jcp

Observation of Penning electron detachment by electronically excited potassium atoms in high Rydberg states

Cite as: J. Chem. Phys. 164, 054312 (2026); doi: 10.1063/5.0311876
Submitted: 12 November 2025 • Accepted: 22 January 2026 •
Published Online: 4 February 2026

Tatsuya Chiba, Moritz Blankenhorn, Shiying Wang, Burak A. Tufekci, Kathryn Foreman, and Kit H. Bowen[a)]

AFFILIATIONS

Department of Chemistry, Johns Hopkins University, Baltimore, Maryland 21218, USA

[a)]Author to whom correspondence should be addressed: kbowen@jhu.edu

ABSTRACT

Penning electron detachment is a process in which an electronically excited neutral species collides with an anion and detaches an electron from it by transferring its excitation energy, viz., $A^- + N^* \rightarrow A + N + e^-$. While there have been theoretical studies relating to the mechanism of Penning detachment, there have been few experimental investigations of this fundamental process. In this work, Penning electron detachment of sulfur pentafluoride anions by potassium atoms, which had been selectively excited to high Rydberg electronic states, was investigated by directly observing its occurrence via the depletion of the SF_5^- anion signal in mass spectra, viz., $SF_5^- + K^{**} \rightarrow SF_5 + K + e^-$. Scanning the excited states of potassium in the range of 8d–32d and 10s–33s (excitation energy 4.11–4.33 eV) showed a significant dependence of the Penning detachment cross section on the excitation energy of potassium. Combining quantitative Penning detachment results with the electron affinity of SF_5 (4.4 eV), which we had determined using anion photoelectron spectroscopy, demonstrated that Penning detachment occurred when the total available energy, that is, the $SF_5^- + K^{**}$ collision energy + the K^{**} excitation energy, exceeded the electron affinity of SF_5.

I. INTRODUCTION

Penning ionization is a well-studied process in which an electronically excited neutral species collides with another neutral species and ionizes it, viz., $A + N^* \rightarrow A^+ + N + e^-$. In analogy with this process, in Penning detachment, a term coined by Blaney and Berry,[1] an electronically excited neutral species collides with an anion and detaches an electron from it, viz., $A^- + N^* \rightarrow A + N + e^-$. While the Penning ionization interaction utilizes the van der Waals attraction between neutral molecules, one of which is electronically excited, the Penning detachment interaction relies on the attraction between an anion and an electronically excited neutral species, making the cross section for Penning detachment larger than that for Penning ionization.[2] Penning electron detachment is relevant to kinetic processes occurring in electric discharges and plasmas as well as in other ionized gas environments,[3] these potentially including magnetically confined plasmas in nuclear fusion reactors.[4] Such collisions may also be important in stellar atmospheres. Our solar atmosphere has an opacity at wavelength <1.6 μm due to the electron photodetachment of H^- ($H^- + h\nu \rightarrow H + e^-$).[5–7] In that highly energetic environment, the Penning electron detachment of H^- by excited hydrogen (or helium) atoms [$H^- + H^*$ (or He^*) $\rightarrow H + H$ (or He) + e^-] is no doubt a competing process with photodetachment. Thus, while sacrificial H^- photodetachment acts to protect us from harmful rays emanating from inside the sun, the Penning detachment of H^- is a process that depletes that protective blanket. Thus, they are both important elementary steps in the overall mechanism. Penning detachment can also be an efficient way of making mass-selected neutral cluster beams.[3]

In the theory of Penning detachment developed by Blaney and Berry in 1971, it was predicted that the Penning detachment cross section should be relatively large due to the attractive interaction between an anion and a highly polarizable, electronically excited neutral.[1] They further developed their theory to calculate the Penning detachment cross sections of H^- by He^*, Li^*, and Ca^* in various electronically excited states.[8,9] These theoretical studies showed

that in some of these anion-excited neutral combinations, the Penning detachment cross section exceeds 10^{-13} cm^2 at low impact energy, with the cross sections depending strongly on the excited state of the neutral species.[8,9] They also extended their theory of Penning detachment to atomic cluster anions [Na_7^-/Na_{19}^- + $Na^*(3p)$] and showed that atomic cluster anions follow the same trend as atomic anions due to the long-range nature of the anion–neutral interaction.[10]

Experimentally, Fehsenfeld *et al.* first observed Penning detachment of O_2^- by $O_2(a\ ^1\Delta_g)$ and measured its reaction rate constant using the flowing afterglow technique in 1969.[11] In 1994, Upschulte *et al.* remeasured the rate constant of this process in an ion flow tube and reported it with a reduced uncertainty.[12] In 2007 and 2008, Midey *et al.* made a further refinement using a selected-ion flow tube and determined its reaction rate to be ~7 × 10^{-10} cm^3 s^{-1} in the temperature range of 200–700 K.[13,14] They attributed the large rate constant to the long-range interaction of the ion and the excited neutral in line with Berry's prediction.[13,14] They further expanded their method to other anions by measuring the rate constants and branching ratios of the reactions, SO_2^- + $O_2(a\ ^1\Delta_g)$ and HO_2^- + $O_2(a\ ^1\Delta_g)$.[15] The astrophysically significant experimental study of the Penning detachment of H^- occurred in 1991, when Dowek *et al.* examined the Penning detachment reaction, H^- + $Na^*(3p)$.[16] There, they accelerated H^- to 0.5–1.5 keV and collided it with $Na^*(3p)$ excited atoms, measuring the energy loss spectrum of neutralized H atoms at each collision energy. Their estimated Penning detachment cross section was 10^{-15} to 10^{-14} cm^2, which is in the range predicted by Berry *et al.*[1,8–10] and 10^2–10^3 times larger than the photodetachment cross section of H^-.[17,18]

In this study, the Penning detachment of sulfur pentafluoride anions, SF_5^-, by Rydberg-excited potassium atoms, K^{**}, was studied by directly observing the depletion of the SF_5^- anion signal in mass spectra. The dependence of the cross section on the excited states of the neutral species was investigated by allowing SF_5^- ions to collide with potassium atoms that had been selectively excited to various [Ar] nd^1 (n = 8–32) and [Ar] ns^1 (n = 10–33) Rydberg electronic states. Rydberg atoms have significant advantages in experimentally observing this phenomenon. Their large volumes (radius ~n^2) and high polarizabilities (~n^7)[19] lead to enhanced collisional cross sections. When interacting with anions, their high polarizabilities lead to large attractive forces due to ion-induced dipole interactions.[1] In addition, their long lifetimes (~n^3)[19] allow the excited potassium atoms time to collide with the anions before their relaxation. By scanning the electronic states of potassium in the range of 8d–32d and 10s–33s Rydberg states, the dependence of the relative Penning detachment cross section on the excitation energy was observed and measured. Combining these Penning detachment results with the electron affinity of SF_5 (4.4 eV), which we determined by anion photoelectron spectroscopy during this study, showed that Penning detachment (SF_5^- + K^{**} → SF_5 + K + e^-) occurred whenever the total available energy (the collision energy of SF_5^- + K^{**} and the electronic excitation energy of K^{**}) exceeded the electron affinity of SF_5.

II. METHODS

These experiments were conducted on an apparatus equipped with four pulsed lasers, a photo-electron-emission anion source, a potassium oven, a time-of-flight mass spectrometer (TOF-MS), and an anion photoelectron spectrometer.[20–22]

A. Penning detachment mass spectral depletion study: SF_5^- + K^{**} → SF_5 + K + e^-

A gas mixture of 10% sulfur hexafluoride/90% helium (~0 psi) was used to generate a supersonic expansion via a pulsed valve (Parker-Hannifin). Electrons produced by laser photoelectron-emission from a rotating/translating copper rod, which was struck at 10 Hz by a Nd:YAG laser beam (Continuum, Surelite II-10, 2nd harmonic, 532 nm), were attached to the effluent SF_6 molecules to produce SF_5^- anions by dissociative electron attachment. Downstream beyond a skimmer, Rydberg-excited potassium atoms, K^{**}, were produced via two-photon excitation by crossing an effusive beam of potassium atoms from an oven (150 °C) with two pulsed dye laser beams. The first laser (Sirah Lasertechnik, Cobra, LDS751 in ethanol, 767 nm) excited the potassium atoms from the ground state to the first excited state ($^2P_{3/2}$ [Ar] $4p^1$), while the second laser (Sirah Lasertechnik, Cobra-Stretch, Coumarin 480 in ethanol, 457–497 nm) further selectively excited them to the various Rydberg electronic states, 8d–32d and 10s–33s. The spin–orbit splitting of the d-Rydberg levels at these high principal quantum numbers were not resolved in our setup. The energy levels of the excited states of potassium were those found in the NIST Atomic Spectra Database.[23] The SF_5^- ion beam was crossed with the resulting Rydberg-excited K^{**} species inside the Wiley–McLaren ion extraction region of a time-of-flight mass spectrometer portion of the greater apparatus, after which they were detected on a microchannel plate (MCP) detector.[24] Mass spectra were measured at each potassium Rydberg level in order to record the depletion of SF_5^- by Penning detachment as a function of the Rydberg electronic states.

To compensate for the shot-to-shot fluctuations of the ion intensity, a timing scheme was devised as shown in Fig. 1. The SF_5^- ion source, the second excitation laser (457–497 nm), and the extraction plates for TOF-MS were pulsed at 10 Hz, while the first excitation laser (767 nm) was pulsed at 5 Hz. In the first cycle in Fig. 1, the first excitation laser was not pulsed; hence, SF_5^- was crossed with ground-state potassium, K. The oscilloscope (GaGe, Compuscope 82G) was triggered 15 μs after the TOF extraction plates were fired. Since the flight time of SF_5^- from the extraction plates to the MCP detector in our apparatus is ~69 μs, this SF_5^- ion signal appeared on the oscilloscope at 69 − 15 μs = 54 μs. In the second cycle, both the first and the second excitation lasers were pulsed so that SF_5^- was crossed with Rydberg-excited potassium atoms, K^{**}. The oscilloscope was triggered simultaneously with the TOF extraction plates, so this SF_5^- ion signal appeared at ~69 μs on the oscilloscope, which is the same as the flight time of SF_5^-. These two cycles were repeated 500 times to accumulate the SF_5^- ion signals that had been crossed with ground state K atoms vs SF_5^- ion signals that had been crossed with Rydberg-excited potassium atoms, K^{**}.

B. Anion photoelectron spectroscopy of SF_5^-

The energy needed to detach an electron from an anion is equal to the electron affinity, EA, of its neutral counterpart. Thus, the EA of SF_5 is the energy required to initiate the Penning detachment of SF_5^-. To determine this value, we performed anion photoelectron spectroscopy by crossing a mass-selected SF_5^- ion beam with

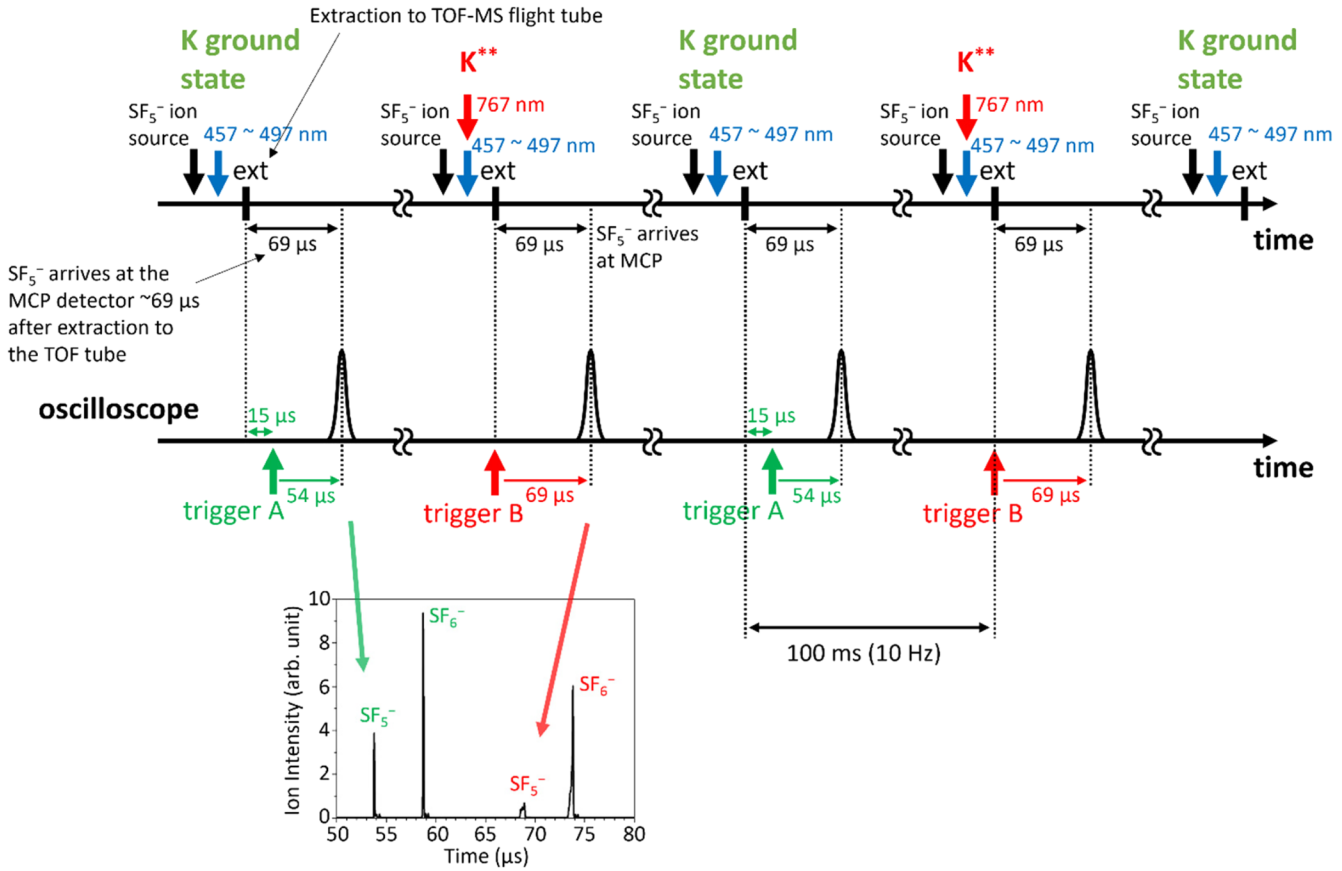

FIG. 1. The timing scheme of the pulsed apparatus' operation and its correspondences with the arrival time of the SF_5^- ion signal. The left side of this figure shows the first two cycles. In the mass spectral inset, the SF_5^- signal appearing at ~54 μs had been crossed with ground-state potassium atoms, while the SF_5^- signal appearing at ~69 μs had been crossed with Rydberg-excited potassium atoms in their 17d Rydberg level and was thus depleted.

193 nm photons from an ArF excimer laser (GAM Laser, EX50F). The kinetic energy of the photodetached electrons was recorded by a magnetic bottle electron energy analyzer, and the binding energy was obtained using the energy conservation relationship, $h\nu$ = EBE + EKE, where $h\nu$ is the photon energy, EBE is the electron binding energy, and EKE is the kinetic energy of the photodetached electron. The resolution of our magnetic bottle is ~35 meV at EKE = 1 eV.[25] The photoelectron spectrum was calibrated by the well-known transitions of Au^-.[26]

To obtain additional information on the SF_5^-/SF_5 system by simulating the experimental aPES, we carried out density functional theory (DFT) calculations. These used the B3LYP functional, an aug-cc-PVDZ basis set for S atom, and a cc-PVDZ basis set for the F atoms, all employing the Gaussian 16 software package.[27] The computed anion photoelectron spectrum was obtained via a Franck–Condon Factor (FCF) analysis.

III. RESULTS

First, let us explain why we focused on the Penning detachment of SF_5^- rather than on that of SF_6^-. During these experiments, neutral SF_6 from the source's pulsed valve interacted with K^{**} to form SF_6^- via Rydberg electron transfer (RET), viz., $SF_6 + K^{**} \rightarrow SF_6^- + K^+$.[20,21] On the other hand, RET did not cause dissociative electron attachment to SF_6 to form SF_5^-, as shown in Fig. S1 in the supplementary material. Thus, while SF_6^- was formed by RET, as an anion, it could also be depleted by Penning detachment, whereas the intensity of SF_5^- could be affected only by its depletion via Penning detachment. Here, we focus on the ion intensity of SF_5^- to study the effect caused solely by Penning detachment. A typical time-of-flight mass spectrum is shown in Fig. 2(a). The two peaks on the left side (~54 and ~59 μs) are $^{31}SF_5^-$ and $^{31}SF_6^-$ crossed with the ground state potassium atoms, while the two peaks on the right side (~69 and ~74 μs) are $^{31}SF_5^-$ and $^{31}SF_6^-$ crossed with the potassium excited to its 17d Rydberg state. The ion intensity of SF_5^- (on the right side) decreased significantly when the potassium was excited to its 17d state by the two excitation lasers. This was due to its Penning detachment. The ion intensity of SF_6^- shown there also showed some, albeit lesser, decrease, and this too was due to its Penning detachment. Figure 2(b) shows the mass spectrum recorded with the potassium oven shut off (flagged), while the excitation lasers continued operating with the same timing as in Fig. 2(a). The fact

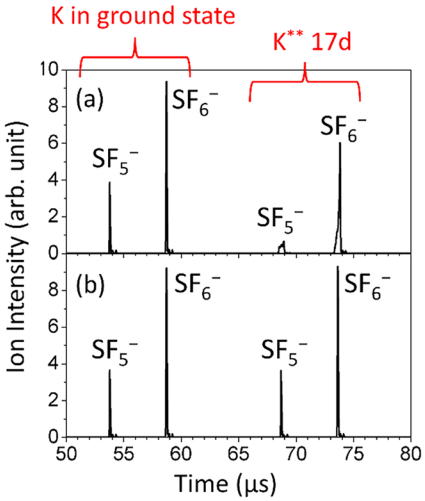

FIG. 2. (a) Time-of-flight mass spectrum of SF_5^- and SF_6^- recorded by the timing scheme shown in Fig. 1. The two peaks on the left (~54 and ~59 μs) show the anions crossed with ground-state potassium, while the two on the right (~69 and ~74 μs) show the anions crossed with potassium excited to the 17d Rydberg level. (b) The same measurement repeated with the potassium oven shut off. Operating the excitation lasers without potassium did not affect the ion intensities.

that operating the two excitation lasers without potassium did not affect the SF_5^- ion intensity confirms that the depletion of SF_5^- in Fig. 2(a) was caused by Penning detachment and not by excitation laser(s)-induced photodetachment.

The same measurements were performed by scanning the Rydberg levels of potassium in the range of 8d–32d and 10s–33s and were repeated in three rounds. The fraction of $^{31}SF_5^-$ depleted by Penning detachment was calculated at each Rydberg level by the following formula and plotted in Fig. 3(a): (Depletion Ratio) = $[(I_{SF_5^-}$ without K^{**} excitation) – $(I_{SF_5^-}$ with K^{**} excitation)$]/(I_{SF_5^-}$ without K^{**} excitation), where $I_{SF_5^-}$ is the ion intensity (TOF peak area) of SF_5^-. In the case of d-Rydberg levels, as much as ~40% of SF_5^- was depleted at 17d–21d, and there is another, albeit smaller, increase in depletion around 30d and 31d. The s-Rydberg levels in Fig. 3(a) showed similar behavior to the d levels, but with lower depletion ratios. This can be attributed to the lower excitation efficiency of potassium to the s-Rydberg levels compared to the d-Rydberg levels. A major reason for this is its lower degeneracy (^{2}S state, degeneracy = 2) compared to that of the d levels (^{2}D state, degeneracy = 10). Note that the observed relative depletion ratios between the s levels and d levels are not a direct reflection of this degeneracy ratio due to other factors, such as the limited number of the K atoms at the interaction region and different excitation efficiency at each level. In Fig. 3(b), the same data were plotted against the excitation energy of potassium. Both d and s levels showed the maximum Penning detachment efficiency around 4.30 eV excitation energy; the small increase in the depletion ratio around 30d and 31d corresponds to an excitation energy of ~4.326 eV.

To determine how much energy is needed to detach an electron from SF_5^-, an anion photoelectron spectrum of SF_5^- was measured, and it is shown in Fig. 4. The vertical detachment energy (VDE), which is the EBE position of the peak maximum in the spectrum, was 5.46 eV. The electron affinity (EA) of SF_5, as estimated as the threshold rise of the electron signal in the anion photoelectron spectrum, was 4.4 eV. By conducting DFT calculations, the computationally determined VDE and adiabatic electron affinity (AEA) values were found to be 5.25 and 4.37 eV, respectively. Figure 4 presents the simulated photoelectron spectrum and compares it with the experimental spectrum. The computed VDE and EA values are in good agreement with the experimental numbers, and the FCF simulation well reproduced the experimental spectrum. The optimized geometry of SF_5^- was found to be square pyramidal, as shown in Fig. S2 in the supplementary material; this is consistent with previous studies.[28,29] The Electron Localization Function (ELF) Natural Bond Orbital (NBO) population analysis in Fig. S3 in the supplementary material shows that the electron density at the S atom is decreased

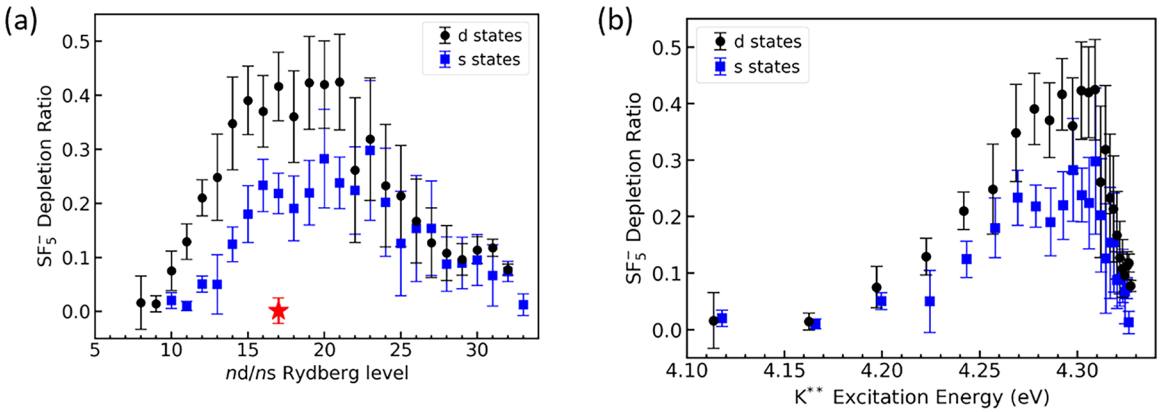

FIG. 3. SF_5^- depletion ratios with the potassium atoms excited to 8d–32d (black) and to 10s–33s (blue) Rydberg states, plotted by (a) the principal quantum number *n* of potassium and (b) the excitation energy of potassium. The red star in (a) is the depletion ratio when the potassium oven was closed, so that no Penning detachment occurred. There, the lasers continued to operate at the wavelength for 17d excitation [corresponding to Fig. 2(b)]. Each measurement was repeated three times, and the error bars represent the standard deviations.

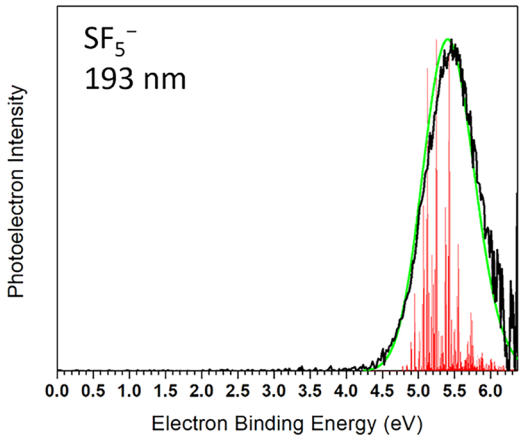

FIG. 4. The anion photoelectron spectrum of SF_5^- recorded with 193 nm photons (black), computed transitions (red sticks), and the simulated spectrum with broadening of FWHM 250 meV (green).

by the transition from SF_5^- to SF_5. The coordinates of the optimized geometries are shown in Tables S1 and S2 in the supplementary material. Although this EA is higher than the values previously estimated from SF_6 experiments,[30–33] anion photoelectron spectroscopy of SF_5^- gives a direct measurement of EA, and the value determined here is in the range of the previous computational predictions.[29,34] Since the excitation energy of K^{**} in our experiment is in the range of 4.11–4.33 eV, which is lower than the EA of SF_5, the excitation energy of K^{**} itself is not enough to induce the Penning detachment of SF_5^-. This indicates that the collision energy also contributed to Penning detachment.

IV. DISCUSSION

To take the collision energy of the SF_5^- + K^{**} Penning detachment reaction into consideration, we begin by estimating the velocities of SF_5^- and K^{**}. The velocity of the effluent stream from a supersonic expansion can be estimated as $v = (5k_BT/m)^{1/2}$, where k_B is the Boltzmann constant, T is the temperature of the gas before expansion, and m is the effective mass of the atoms and molecules in the gas.[35] By using $T = 300$ K (room temperature) and $m = 18.2$ amu (the average mass of the 10% SF_6/90% He gas mixture), the speed of SF_5^- is estimated to be $v_{SF_5^-} = 828$ m/s. The speed of the effusive beam of K atoms from the 150 °C oven follows the Maxwell–Boltzmann distribution [Fig. 5(a) for ^{39}K]; $P(v_K)dv_K = 4\pi(m_K/(2\pi k_BT))^{3/2}v_K^2 \exp\left(-mv_K^2/(2k_BT)\right)dv_K$. The collision energy of $^{31}SF_5^-$ + K^{**} can be calculated by $E_{collision} = (1/2)\mu|\vec{v}_{rel}|^2 = (1/2)\mu\left(v_K^2 + v_{SF_5^-}^2\right)$, where μ is the

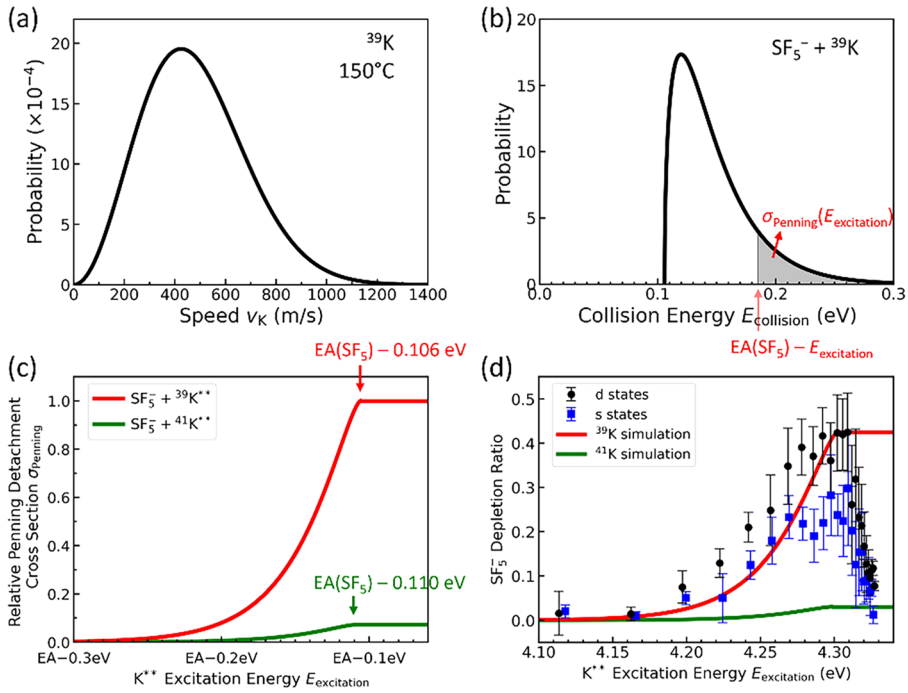

FIG. 5. (a) The Maxwell–Boltzmann speed distribution of the effusive beam of ^{39}K atoms from a 150 °C oven. (b) The distribution of the collision energy $E_{collision}$ for the collision between a supersonic beam of SF_5^- (828 m/s) and an effusive beam of ^{39}K (150 °C) at a right angle. For the shaded area representing $\sigma_{Penning}(E_{excitation})$, the $E_{excitation}$ was set to be 4.223 eV (K^{**} 11d) as an example. (c) Modeled relative Penning detachment cross section as a function of the K^{**} excitation energy $\sigma_{Penning}(E_{excitation})$ for ^{39}K (red) and ^{41}K (green). The graph of ^{41}K is scaled by the isotopic natural abundance ratio (^{39}K:^{41}K = 100:7.2).[36] $\sigma_{Penning}(E_{excitation})$ for ^{39}K and ^{41}K plateaus at slightly different energies due to the different reduced masses for SF_5^- + ^{39}K and SF_5^- + ^{41}K collisions. (d) The modeled relative Penning detachment cross section $\sigma_{Penning}(E_{excitation})$ overlaid on the experimental data shown in Fig. 3(b), so that $\sigma_{Penning}(E_{excitation})$ reaches its maximum at 19d ($E_{excitation}$ = 4.302 eV), that is, setting the EA(SF_5) to be 4.408 eV.

reduced mass, and $\vec{v}_{rel}$ is the relative velocity, when the two species are colliding at a right angle. The distribution of the collision energy based on the Maxwell speed distribution of K atoms is $P(E_{collision}) = P(v_K) \cdot (dv_K/dE_{collision})$, where $dv_K/dE_{collision} = 1/(\mu v_K)$ is the Jacobian to convert the variable of the Maxwell's probability distribution function from speed (v_K) to energy ($E_{collision}$). This collision energy distribution is shown in Fig. 5(b) for ^{39}K. Here, we assume that Penning detachment occurs when the total available energy (total of the collision energy $E_{collision}$ and the K** excitation energy $E_{excitation}$) exceeds the EA of SF_5 [$E_{collision} + E_{excitation} > EA(SF_5)$]. At a given excitation energy, Penning detachment occurs when the collision energy exceeds $EA(SF_5) - E_{excitation}$. This corresponds to the shaded area in Fig. 5(b) in the case of ^{39}K** at the 11d Rydberg level ($E_{excitation}$ = 4.223 eV), and this area can be seen as the relative Penning detachment cross section as a function of the excitation energy of the neutral species $\sigma_{Penning}(E_{excitation})$. A plot of $\sigma_{Penning}(E_{excitation})$ is shown in Fig. 5(c). $\sigma_{Penning}$ reaches its maximum and plateaus at $E_{excitation} = EA(SF_5) - 0.106$ eV, where all $SF_5^- + {}^{39}K^{**}$ collisions satisfy the energetic requirement of Penning detachment [$E_{collision} + E_{excitation} > EA(SF_5)$]. In the experimental data in Fig. 3(b), the Penning detachment cross section reached its maximum at 19d and plateaued through 21d. Figure 5(d) shows the graph of $\sigma_{Penning}(E_{excitation})$ overlaid on the experimental SF_5^- depletion ratio, so that $\sigma_{Penning}(E_{excitation})$ reaches its maximum at 19d ($E_{excitation}$ = 4.302 eV), that is, the $EA(SF_5)$ set to be 4.408 eV. The modeled $\sigma_{Penning}(E_{excitation})$ well reproduced the experimentally observed behavior of the relative Penning detachment cross section up to 21d ($E_{excitation}$ = 4.309 eV). The EA of SF_5 (4.408 eV) obtained from this Penning detachment discussion agrees with the EA obtained from the anion photoelectron spectrum in Fig. 4. This picture of the energetic requirement is also consistent with the broadening of the SF_5^- ion signal by K** in Fig. 2(a). In the intermediate K** Rydberg levels, including 17d, the slow K** atoms do not have enough collision energy to cause Penning detachment [corresponding to the unshaded area in Fig. 5(b)]. In that case, while the $SF_5^- + K^{**}$ collisions do not lead to Penning detachment, the momentum of SF_5^- is changed by the collision, and this causes the observed broadening in the Wiley–McLaren-type, time-of-flight mass spectrum.

At the 22d Rydberg level and above, the experimental Penning detachment cross section decreased although it satisfied the energetic requirement. This may have been because K** was ionized by the collision with SF_5^- or SF_6, due to the small ionization energy (<29 meV) at these highly excited states. Another possibility is that the photon emission from K** ($SF_5^- + K^{**} \rightarrow SF_5^- + K^{(*)} + h\nu$) competed with Penning detachment.[1] At these high Rydberg levels, the energy spacings between the neighboring electronic states with different orbital angular momenta are extremely narrow. Stark mixing of these neighboring states, induced by the approaching electric field of SF_5^-, could open new decay channels for K**. For example, 22d has a neighboring level of 23p within 1.3 meV.[37] Mixing of these two levels opens a channel for K**(22d) to decay to the ground state K(4s) by photon emission with the allowed transition of $\Delta l = \pm 1$. While further investigation is needed to reveal whether the sharp decrease of the depletion ratio at the high excitation energy end is caused by the K** ionization or photon emission, the agreement between the experimental data and the energy-based model up to 4.30 eV in Fig. 5(d) indicates that these effects are pronounced only at the high excitation energy/low ionization energy end of K**, and they rapidly diminish at the lower excitation energy. Quantitative evaluation of these effects might explain the small increase of the observed depletion ratio around the excitation energy of 4.326 eV (30d and 31d).

V. CONCLUSION

In summary, Penning detachment of SF_5^- by potassium atoms in high Rydberg electronic states was observed by scanning the excitation energy of potassium atoms in the range of 4.11–4.33 eV (8d–32d, 10s–33s). The modeled Penning detachment cross section, based on the energetic requirement, reproduced the increase of the experimentally observed Penning detachment cross section as the excitation energy increased. The agreement between the modeled and experimental Penning detachment behavior and the electron affinity of SF_5 (4.4 eV), determined by anion photoelectron spectroscopy, revealed that Penning detachment ($SF_5^- + K^{**} \rightarrow SF_5 + K + e^-$) occurred when the total available energy, which includes the $SF_5^- + K^{**}$ collision energy and the K** excitation energy, exceeded the electron affinity of SF_5. This is the first experimental study that provides insights into the mechanisms of Penning detachment with unambiguous observation of its occurrence. Further investigations of Penning detachment using different anion/excited neutral combinations will be helpful to better understand the mechanisms. One of the most important systems for future study is the Penning detachment from H^-, due to its role in stellar atmospheres and nuclear fusion reactors.

SUPPLEMENTARY MATERIAL

See the supplementary material for Figs. S1–S3, and Tables S1 and S2.

ACKNOWLEDGMENTS

Our studies of Penning detachment were inspired by our conversations with the late Steve Berry. This material is based on work supported by the Air Force Office of Scientific Research (AFOSR) under Grant Number FA9550-22-1-0271 (K.H.B.).

AUTHOR DECLARATIONS

Conflict of Interest

The authors have no conflicts to disclose.

Author Contributions

T.C., M.B., S.W., and K.F. performed the mass spectral study. S.W., B.A.T., and T.C. performed the anion photoelectron spectroscopy. B.A.T. performed the DFT calculations. K.H.B. supervised the work. T.C. and M.B. contributed equally to this work.

Tatsuya Chiba: Data curation (equal); Formal analysis (equal); Investigation (equal); Methodology (equal); Writing – original draft (equal). **Moritz Blankenhorn**: Data curation (equal); Formal analysis (equal); Investigation (equal); Methodology (equal); Writing – original draft (equal). **Shiying Wang**: Data curation (equal); Investigation (equal). **Burak A. Tufekci**: Data curation (equal); Investigation (equal). **Kathryn Foreman**: Data curation (equal); Investigation (equal). **Kit H. Bowen**: Conceptualization (lead); Funding acquisition (lead); Investigation (lead); Methodology (lead); Project administration (lead); Resources (lead); Supervision (lead); Writing – review & editing (lead).

DATA AVAILABILITY

The data that support the findings of this study are available from the corresponding author upon reasonable request.

REFERENCES

[1] B. Blaney and R. S. Berry, Phys. Rev. A **3**, 1349 (1971).
[2] R. S. Berry, Phys. Chem. Chem. Phys. **7**, 286 (2005).
[3] R. S. Berry, The Air Force Office of Scientific Research, Final Technical Report, Grant No. AFOSR-89-0256, 1993.
[4] J. Wesson, *Tokamaks*, 4th ed. (Oxford University Press, New York, 2011).
[5] R. Wildt, Astrophys. J. **90**, 611 (1939).
[6] T. J. Millar, C. Walsh, and T. A. Field, Chem. Rev. **117**, 1765 (2017).
[7] N. J. Woolf, M. Schwarzschild, and W. K. Rose, Astrophys. J. **140**, 833 (1964).
[8] F. Martín and R. S. Berry, Phys. Rev. A **55**, 1099 (1997).
[9] F. Martín and R. S. Berry, Phys. Rev. A **55**, 4209 (1997).
[10] F. Martín, M. E. Madjet, P. A. Hervieux, J. Hanssen, M. F. Politis, and R. S. Berry, J. Chem. Phys. **111**, 8934 (1999).
[11] F. C. Fehsenfeld, D. L. Albritton, J. A. Burt, and H. I. Schiff, Can. J. Chem. **47**, 1793 (1969).
[12] B. L. Upschulte, W. J. Marinelli, and B. D. Green, J. Phys. Chem. **98**, 837 (1994).
[13] A. Midey, I. Dotan, S. Lee, W. T. Rawlins, M. A. Johnson, and A. A. Viggiano, J. Phys. Chem. A **111**, 5218 (2007).
[14] A. Midey, I. Dotan, and A. A. Viggiano, J. Phys. Chem. A **112**, 3040 (2008).
[15] A. Midey, I. Dotan, J. V. Seeley, and A. A. Viggiano, Int. J. Mass Spectrom. **280**, 6 (2009).
[16] D. Dowek, J. C. Houver, C. Richter, and N. Andersen, Z. Phys. D: At., Mol. Clusters **18**, 231 (1991).
[17] L. M. Branscomb and S. J. Smith, Phys. Rev. **98**, 1028 (1955).
[18] M. Génévriez and X. Urbain, Phys. Rev. A **91**, 033403 (2015).
[19] T. F. Gallagher, Rep. Prog. Phys. **51**, 143 (1988).
[20] S. M. Ciborowski, R. M. Harris, G. Liu, C. J. Martinez-Martinez, P. Skurski, and K. H. Bowen, Jr., J. Chem. Phys. **150**, 161103 (2019).
[21] G. Liu, S. M. Ciborowski, J. D. Graham, A. M. Buytendyk, and K. H. Bowen, J. Chem. Phys. **151**, 101101 (2019).
[22] A. M. Buytendyk, J. D. Graham, K. D. Collins, K. H. Bowen, C.-H. Wu, and J. I. Wu, Phys. Chem. Chem. Phys. **17**, 25109 (2015).
[23] A. Kramida, Y. Ralchenko, J. Reader, and NIST ASD Team, *NIST Atomic Spectra Database, ver. 5.10* (National Institute of Standards and Technology, Gaithersburg, 2023).
[24] W. C. Wiley and I. H. McLaren, Rev. Sci. Instrum. **26**, 1150 (1955).
[25] X. Zhang, G. Liu, G. Ganteför, K. H. Bowen, and A. N. Alexandrova, J. Phys. Chem. Lett. **5**, 1596 (2014).
[26] J. Ho, K. M. Ervin, and W. C. Lineberger, J. Chem. Phys. **93**, 6987 (1990).
[27] M. J. Frisch, G. W. Trucks, H. B. Schlegel, G. E. Scuseria, M. A. Robb, J. R. Cheeseman, G. Scalmani, V. Barone, G. A. Petersson, H. Nakatsuji, X. Li, M. Caricato, A. V. Marenich, J. Bloino, B. G. Janesko, R. Gomperts, B. Mennucci, H. P. Hratchian, J. V. Ortiz, A. F. Izmaylov, J. L. Sonnenberg, D. Williams-Young, F. Ding, F. Lipparini, F. Egidi, J. Goings, B. Peng, A. Petrone, T. Henderson, D. Ranasinghe, V. G. Zakrzewski, J. Gao, N. Rega, G. Zheng, W. Liang, M. Hada, M. Ehara, K. Toyota, R. Fukuda, J. Hasegawa, M. Ishida, T. Nakajima, Y. Honda, O. Kitao, H. Nakai, T. Vreven, K. Throssell, J. A. Montgomery, Jr., J. E. Peralta, F. Ogliaro, M. J. Bearpark, J. J. Heyd, E. N. Brothers, K. N. Kudin, V. N. Staroverov, T. A. Keith, R. Kobayashi, J. Normand, K. Raghavachari, A. P. Rendell, J. C. Burant, S. S. Iyengar, J. Tomasi, M. Cossi, J. M. Millam, M. Klene, C. Adamo, R. Cammi, J. W. Ochterski, R. L. Martin, K. Morokuma, O. Farkas, J. B. Foresman, and D. J. Fox, *Gaussian 16, Revision C.02*, Gaussian, Inc., Wallingford, CT, 2019.
[28] K. O. Christe, E. C. Curtis, C. J. Schack, and D. Pilipovich, Inorg. Chem. **11**, 1679 (1972).
[29] T. Ziegler and G. L. Gutsev, J. Chem. Phys. **96**, 7623–7632 (1992).
[30] R. N. Compton and C. D. Cooper, J. Chem. Phys. **59**, 4140 (1973).
[31] R. N. Compton, P. W. Reinhardt, and C. D. Cooper, J. Chem. Phys. **68**, 2023 (1978).
[32] E. C. M. Chen, L.-R. Shuie, E. D. D'sa, C. F. Batten, and W. E. Wentworth, J. Chem. Phys. **88**, 4711 (1988).
[33] E. C. M. Chen and E. S. Chen, Phys. Rev. A **76**, 032508 (2007).
[34] R. Mane, N. Mehrotra, D. K. Maity, and A. K. Gupta, Rapid Commun. Mass Spectrom. **29**, 1317 (2015).
[35] P. L. Houston, *Chemical Kinetics and Reaction Dynamics* (The McGraw-Hill Companies, Inc., New York, 2001), pp. 264–265.
[36] J. E. Sansonetti and W. C. Martin, *Handbook of Basic Atomic Spectroscopic Data*, *NIST Standard Reference Database 108* (National Institute of Science and Technology, Gaithersburg, 2024).
[37] C. Corliss and J. Sugar, J. Phys. Chem. Ref. Data **8**, 1109 (1979).